# A Role of Tyrosine Phosphatase in Acetylcholine Receptor Cluster Dispersal and Formation

**Zhengshan Dai and H. Benjamin Peng**

Department of Cell Biology and Anatomy and the Curriculum in Neurobiology, University of North Carolina, Chapel Hill, North Carolina 27599-7090

***Abstract.*** Innervation of the skeletal muscle involves local signaling, leading to acetylcholine receptor (AChR) clustering, and global signaling, manifested by the dispersal of preexisting AChR clusters (hot spots). Receptor tyrosine kinase (RTK) activation has been shown to mediate AChR clustering. In this study, the role of tyrosine phosphatase (PTPase) in the dispersal of hot spots was examined. Hot spot dispersal in cultured *Xenopus* muscle cells was initiated immediately upon the presentation of growth factor–coated beads that induce both AChR cluster formation and dispersal. Whereas the density of AChRs decreased with time, the fine structure of the hot spot remained relatively constant. Although AChR, rapsyn, and phosphotyrosine disappeared, a large part of the original hot spot–associated cytoskeleton remained. This suggests that the dispersal involves the removal of a key linkage between the receptor and its cytoskeletal infrastructure. The rate of hot spot dispersal is inversely related to its distance from the site of synaptic stimulation, implicating the diffusible nature of the signal. PTPase inhibitors, such as pervanadate or phenylarsine oxide, inhibited hot spot dispersal. In addition, they also affected the formation of new clusters in such a way that AChR microclusters extended beyond the boundary set by the clustering stimuli. Furthermore, by introducing a constitutively active PTPase into cultured muscle cells, hot spots were dispersed in a stimulus-independent fashion. This effect of exogenous PTPase was also blocked by pervanadate. These results implicate a role of PTPase in AChR cluster dispersal and formation. In addition to RTK activation, synaptic stimulation may also activate PTPase which acts globally to destabilize preexisting AChR hot spots and locally to facilitate AChR clustering in a spatially discrete manner by countering the action of RTKs.

THE clustering of neurotransmitter receptors is a key event during the development of the synapse (12, 19, 26, 32, 52). The reverse process, the disassembly of receptor clusters, is associated with plastic changes in synaptic structure (10). This is best illustrated by the formation of the vertebrate neuromuscular junction (NMJ).[1] During embryonic development, motoneuron processes make contact with muscle fibers and induce the formation of acetylcholine receptor (AChR) clusters at the nerve–muscle contact (26). During the subsequent process of the elimination of polyneuronal innervation, AChR clusters underneath noncompeting nerve terminals are dismantled and this is followed by the retraction of these terminals (6, 10). An analogous process is observed in cultured muscle cells. When they are innervated by spinal cord neurons, AChRs become clustered at the nerve–muscle contact and preexisting AChR clusters (hot spots) undergo dispersal (31, 39, 41). This demonstrates that innervation produces two kinds of effect on the muscle cell: a local effect as shown by AChR clustering in the subsynaptic area and a global effect exemplified by hot spot dispersal in the extrajunctional region.

Recent studies have shown that the formation of AChR clusters is mediated by tyrosine kinase activation as a result of the presentation of synaptogenic signals such as agrin and growth factors to the muscle (5, 15, 55, 58). The muscle-specific kinase (MuSK, also known as Nsk2) appears to mediate the agrin-induced AChR clustering (21, 25). Although the cellular events after the kinase activation have not been elucidated, previous studies have shown that the assembly of a cytoskeleton specialization is an integral part of the clustering process (8, 18). Both structural proteins and kinases have been shown to be as-

Address correspondence to Dr. H. Benjamin Peng, University of North Carolina, Department of Cell Biology and Anatomy, CB#7090, Chapel Hill, NC 27599-7090. Tel.: (919) 966-1338. Fax: (919) 966-1856. E-mail: unchbp@med.unc.edu

1. *Abbreviations used in this paper*: AChR, acetylcholine receptor; FAK, focal adhesion kinase; HB-GAM, heparin-binding growth-associated molecule; MuSK, muscle-specific kinase; NMJ, neuromuscular junction; PAO, phenylarsine oxide; PTPase, tyrosine phosphatase; PV, pervanadate; R-BTX, rhodamine-conjugated α-bungarotoxin; RTK, receptor tyrosine kinase.

sociated with AChR-rich postsynaptic cytoskeleton (4, 18, 54). Some of these proteins, such as rapsyn (43K protein), are directly involved in cluster formation, whereas others may become concentrated after receptor accumulation.

In contrast to its assembly, the process of AChR cluster dispersal is not understood. What is the nature of the signal emanating from the site of new cluster formation in causing destabilization and disassembly of preexisting AChR hot spots? Does the dispersal involve a dismantling of the entire postsynaptic cytoskeleton? In this study, we attempted to answer these questions by using cultured muscle cells as a model. Both spinal cord neurons and growth factor–coated beads were used as stimuli for AChR clustering (43, 44). Our previous studies have shown that these beads mimic the neuron in inducing both formation and dispersal of AChR clusters (41, 43). By examining clusters undergoing disassembly, we found that the dispersal involves the removal of a link between the receptor and the postsynaptic cytoskeleton, which remains largely intact after receptors are vacated. As tyrosine phosphorylation is a key event in the formation of the clusters, we reasoned that the reverse process of tyrosine dephosphorylation may be involved in their dispersal. This was tested through the use of tyrosine phosphatase (PTPase) inhibitors and direct microinjection of constitutively active PTPase. Through these studies, we found that PTPase plays an important role in cluster dispersal as well as in its formation.

## Materials and Methods

### Materials

Rhodamine-conjugated α-bungarotoxin (R-BTX) and fluorescein-conjugated dextran were purchased from Molecular Probes, Inc. (Eugene, OR). Oregon green–conjugated α-bungarotoxin was provided by Dr. Richard Rotundo (University of Miami, FL). Sodium orthovanadate and phenylarsine oxide (PAO) were from Sigma Chemical Co. (St. Louis, MO). Recombinant *Yersinia* PTPase (51-kD catalytic domain) was from Calbiochem-Novabiochem Corp. (La Jolla, CA). The following antibodies were used in this study: rapsyn, mAb 1234; dystrophin, mAb 1958; syntrophin, mAb 1351 (these three antibodies provided by Dr. Stan Froehner, University of North Carolina); phosphotyrosine, mAb 4G10 (Upstate Biotechnology, Lake Placid, NY); utrophin, BH11 (provided by Dr. T. Kharana, Harvard Medical School, Boston, MA); FAK, mAb 2A7 (provided by Dr. Tom Parsons, University of Virginia, VA). These antibodies have been shown to label *Xenopus* muscle cells specifically (4, 5, 20, 47, 48). Fluorescently conjugated secondary antibodies were purchased from Organon-Teknika Cappel (Durham, NC). Heparin-binding growth-associated molecule (HB-GAM) was a gift of Dr. Heikki Rauvala (University of Helsinki, Finland).

### Cell Culture and AChR Cluster Induction

Neurons and muscle cells were isolated from *Xenopus* embryos according to a published method (45). They were plated on glass coverslips and cultured in Steinberg medium (60 mM NaCl, 0.7 mM KCl, 0.4 mM $Ca(NO_3)_2$, 0.8 mM $MgSO_4$, 10 mM Hepes, pH 7.4, plus 10% L-15, 1% fetal bovine serum, and 0.1 mg/ml gentamicin). The cultures were maintained at 22°C for 24 h and then transferred into a 15°C incubator before being used for experiments. To study the formation of the NMJ, neurons were seeded into muscle cultures 3 d after plating. AChR clusters can be detected at nerve–muscle contacts after 24 h of coculture. AChR clustering was also induced by beads coated with HB-GAM, a growth factor bound to the heparan-sulfate proteoglycan on the surface of *Xenopus* muscle cells (43). Polystyrene latex beads 10 μm in diameter were washed with 95% ethanol and incubated with recombinant HB-GAM at a concentration of 100 μg/ml for several hours, washed and applied to cultured muscle cells. AChR clusters, formed discretely at bead–muscle contacts, can be detected within 24 h of bead application.

### Fluorescent Labeling and Digital Video Microscopy

To visualize AChR clusters, muscle cells were labeled with 30 nM R-BTX for 30 min and examined with a Zeiss IM-35 inverted fluorescence microscope equipped with a 100× objective (NA 1.32) in the living state. For the study on nerve-induced hot spot dispersal, Oregon green–conjugated α-bungarotoxin was used and the specimen was examined with fluorescein filter set. Images were acquired with a Hamamatsu C2400 silicone-intensified target (SIT) camera interfaced with Metamorph image acquisition and analysis software (Universal Imaging Corp., West Chester, PA). The images were analyzed off-line with the same software. To follow the dispersal and the formation of AChR clusters, the same muscle cell was repeatedly imaged over a period of 24 to 48 h. In this case, neutral-density filters, which reduce the excitation to as little of 1% of the normal level, were used to minimize photobleaching and photodamage to the cells.

For antibody labeling, cultured *Xenopus* muscle cells were first labeled with R-BTX and AChR hot spots on selected cells were mapped by digitized fluorescence microscopy. The cultures were then treated with HB-GAM–coated beads to induce the formation of new clusters. 24 h after bead addition, previously recorded cells were reexamined to document the dispersal of preexistent hot spots. The cultures were then fixed and permeabilized with 95% ethanol, and labeled with specific antibodies for different postsynaptic proteins followed by fluorescently conjugated secondary antibody. Previously imaged cells were reexamined with a Leitz Orthoplan fluorescence microscope equipped with a 63× objective (NA 1.4). Images were acquired with a Hamamatsu C5985 chilled CCD camera interfaced with the Metamorph software.

To obtain three-dimensional information of AChR clusters, a stack of images along the optical axis were acquired with the aid of a computer-controlled focusing stepping motor. The image stacks were processed with a dehazing program within the Metamorph software to remove the out-of-focus haze. The image stack was then projected at different angles and digitally enhanced. This allowed us to study the fine structure of hot spots from different viewing angles. The digital images were imported to Corel Draw software (Ottawa, Ontario, Canada) for the assembly into figures used in this paper.

To quantify the fluorescence intensity of hot spots, the mean intensity of a hot spot area above certain threshold was measured. The background fluorescence was then subtracted from the mean. The threshold was adjusted for each hot spot at each time point during the time-lapse recording to keep the total number of hot spot pixels with gray levels above the threshold constant. This adjustment is necessary to avoid overestimating the intensity of dispersing hot spot due to the dwindling of measuring area if a fixed threshold is applied. The fluorescence intensity of individual hot spot was plotted as a function of time and fitted with a simple exponential decay curve using SigmaPlot software (Jandel Scientific, San Rafael, CA).

### PTPase Inhibitor Application

Two PTPase inhibitors were used in this study. Pervanadate (PV) was prepared according to previously published method (58). In brief, 2 μl of 500 mM $H_2O_2$ was mixed with 100 ml of 10 mM sodium orthovanadate for 10 min just before application. The experimental solution was made by diluting this stock solution with culture medium to final concentrations. PAO (22) was first made into 10 mM stock in DMSO. It was then diluted with culture medium to make the experimental solution.

### Introduction of Exogenous PTPase into Muscle Cells

Since *Xenopus* muscle cells contract in response to the slightest mechanical injury associated with micropipette impaling, an alternative method based on patch-clamping was used to deliver PTPase into these cells. The patch clamp pipette was drawn and polished according to standard method (27) with Narishige (Tokyo, Japan) micropipette puller and microforge. The pipette tip was first filled with a small amount of the intracellular recording buffer (60 mM KCl, 4 mM $MgCl_2$, 10 mM K-EGTA, 10 mM Hepes, pH 7.4) by suction. Then, the pipette was back-filled with this buffer plus 3 IU/μl *Yersinia* PTPase and 2.5 μg/μl FITC-dextran. Once the gΩ seal was formed between the pipette and the cell membrane, the holding potential was adjusted to −80 mV to prevent the contraction of the muscle cell while the membrane underneath the pipette was broken by suction to establish the whole-cell recording mode. An EPC-7 patch-clamp amplifier (List-Electronic, Darmstadt/Eberstadt, Germany) was

used to conduct the recording. The pipette was maintained on the cell for 2 min to allow the diffusion of the enzyme and the fluorescent marker into the cell. It was then carefully withdrawn to ensure the resealing of the membrane. After this procedure, muscle cells remained healthy for at least 24 h as shown by the retention of fluorescent marker and their capability to form bead-induced AChR clusters in control cells loaded with dye only as well as the persistence of cross striations.

To quantify the dispersal of hot spots in injected cells, their mean fluorescence intensity minus background was measured with methods described above. The value was then normalized with the intensity of hot spots on neighboring uninjected muscle cells. This procedure is described by the following equation:

$$I_{inj}(N) = ([I_{inj} - I_b] / [I_{nb} - I_b]) \times 100\%$$

where $I_{inj}(N)$ and $I_{inj}$ are normalized, and mean measured intensity of the hot spot in the injected cell, $I_{nb}$ is the mean measured intensity of hot spots in neighboring cells, and $I_b$ is the mean intensity of the background, respectively.

## Results

### Dispersal of AChR Hot Spots

AChRs become spontaneously clustered into hot spots in the absence of NMJ-inducing signals from motoneurons both in vivo and in vitro (2, 23, 33). When motoneuron processes come into contact with the muscle cell, they induce the formation of new clusters at the nerve–muscle contact area and cause the dispersal of preexisting hot spots (26, 31, 39). Both effects of innervation can be mimicked by polystyrene latex beads coated with HB-GAM in cultured *Xenopus* muscle cells (43). Bead stimulation allows accurate determination of the timing and the location of AChR clustering. As shown in Fig. 1 *A*, AChR clustering at bead–muscle contacts evidenced by labeling with R-BTX

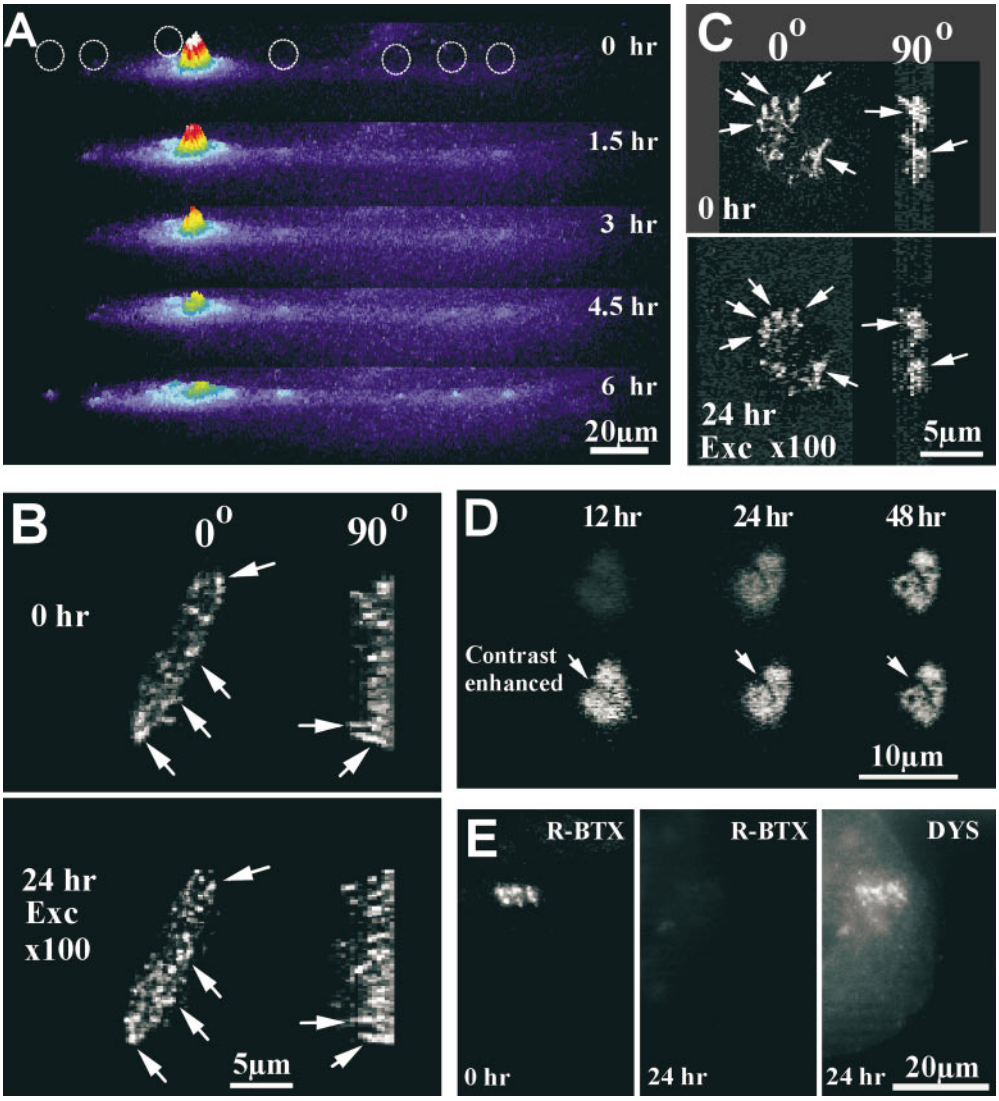


*Figure 1.* AChR cluster dispersal and formation captured with digital video microscopy. (*A*) Time-lapse recording of a muscle cell labeled with R-BTX. The fluorescence intensity, which reflects the AChR density, is represented by both height and pseudocolor. The dispersal of the hot spot was induced by HB-GAM–coated beads whose positions are marked by dotted circles. New AChR clusters formed underneath the beads while the preexisting hot spot to the left underwent dispersal. (*B* and *C*) Preservation of the fine structure of hot spots during the dispersal process. The images were taken before and 24 h after bead addition. To record the hot spot at 24 h, the excitation light was increased 100× by the removal of neutral-density filters. Comparison of images at these two time points shows that only 1% AChRs still remained at the original hot spot, which is shown from the top and from the side (90° rotation). The arrows point to fine-structural features that were preserved during this period of time. (*D*) Persistence of the fine structure of a developing AChR cluster. This cluster was induced by a HB-GAM–coated bead. The top panels show unaltered images of this cluster and the bottom panels show the same images that were contrast enhanced. The fine structure of the cluster at the early stage of formation is largely conserved throughout the process. The arrow points to a groove in the cluster which persisted at all stages. (*E*) Dystrophin localization at a dispersed AChR hot spot. After acquiring the image of the hot spot at time zero (R-BTX, 0 h), beads were added to the muscle cell to induce its dispersal. The image at 24 h shows that this cluster was dispersed. The culture was then fixed and labeled with anti-dystrophin antibody. As shown here, dystrophin remained concentrated at the original hot spot site (DYS, 24 h).

labeling became visible within 3 h after bead application. Concomitant with receptor clustering, the preexisting hot spots away from beads were dispersed (Fig. 1 A).

To understand the mechanism of AChR cluster dispersal, structural changes of hot spots undergoing disassembly were examined. By optically sectioning through the hot spot, its three-dimensional structure can be reconstructed as shown in Fig. 1 *B*. By digitally rotating the hot spot to obtain views at different angles, it became clear that AChRs are clustered both at the surface of the muscle cell as well along the membrane invaginations which can be up to 5 μm in length (*arrows* in Fig. 1 B, 0 h, 90°). Using this method, we followed the dispersal of 11 hot spots from 10 muscle cells induced by HB-GAM–coated beads. We found that there was a high degree of conservation in the fine-structural features of hot spots throughout the dispersal process, as shown in the two examples in Fig. 1, *B* and *C*. Even though the density of AChRs was diminished to ~1% of the original at the end of the 24 h dispersal period as shown by the drop in R-BTX labeling intensity, structural details could still be correlated with features present at the intact cluster at time zero (*arrows* in Fig. 1, *B* and *C*). This suggests the existence of a relatively stable scaffold at the hot spot upon which AChRs are reversibly attached.

To further test this idea, the formation of 12 bead-induced AChR clusters from 5 muscle cells was followed over a period of 48 h. As shown in the example in Fig. 1 *D*, the fine structure of each new cluster was also preserved as it developed despite a gradual increase in AChR density. Thus, the scaffold, which presumably consists of a complex of cytoskeletal proteins, is established early as a result of synaptogenic stimulation and the clustering involves recruitment of receptors to the site of this specialization. The dispersal, on the other hand, involves the removal of a key link between AChR and this cytoskeleton without dismantling of the entire apparatus.

Previous studies have shown that AChR clusters are associated with a number of structural and regulatory proteins (8, 18, 26). To understand which ones are preserved at the original hot spot site after AChR dispersal, immunofluorescence studies were conducted on identified hot spots after their dispersal. As listed in Table I, out of a total of seven markers which are known to be concentrated at hot spots, only three, including AChR, rapsyn and phosphotyrosine, were dispersed, as shown by the decrease in the immunofluorescence intensity to <1% the control value in unperturbed cells. The other markers, including dystrophin, syntrophin, utrophin and focal adhesion kinase (FAK), remained clustered at original hot spot sites for the duration of the experiment. An example of dystrophin preserved at a dispersed hot spot is shown in Fig. 1 *E*. The intensity of the labeling shows no detectable difference from that at an unperturbed hot spot. These latter proteins, though concentrated at the cluster, generally showed more extensive distribution than AChRs, while rapsyn or phosphotyrosine labeling was congruent with that of AChRs (Table I). This suggests that proteins such as dystrophin, utrophin, or syntrophin are involved in the assembly and maintenance of the underlying cytoskeletal complex but are not involved in anchoring AChRs. Thus, the cluster dispersal seems to involve the relatively minor act of disconnecting AChRs from the cytoskeletal scaffold.

*Table I. AChR and Its Related Proteins at Hot Spots Before and After Dispersal*

| Marker | Present at hot spot | Correlation with hot spot | Present at dispersed hot spot |
|---|---|---|---|
| AChR | Yes | Exact | No |
| Rapsyn (43K protein) | Yes | Exact | No |
| Phosphotyrosine | Yes | Exact | No |
| Dystrophin | Yes | More extensive than AChRs | Yes |
| Utrophin | Yes | More extensive than AChRs | Yes |
| Syntrophin | Yes | More extensive than AChRs | Yes |
| Focal adhesion kinase (FAK) | Yes | More extensive than AChRs | Yes |

Cultured *Xenopus* muscle cells were labeled with R-BTX and AChR hot spots on selected cells were mapped by digitized fluorescence microscopy. The cultures were then treated with HB-GAM–coated beads to induce the formation of new clusters. 24 h after bead addition, previously recorded cells were reexamined to document the dispersal of preexistent hot spots. The cultures were then fixed, permeabilized, and labeled with specific antibodies for different postsynaptic proteins followed by fluorescently conjugated secondary antibody. The following antibodies were used in this study: rapsyn, monoclonal antibody (mAb) 1234; dystrophin, mAb 1958; syntrophin, mAb 1351; phosphotyrosine, mAb 4G10; utrophin, BH11; FAK, mAb 2A7. These antibodies were previously tested on *Xenopus* muscle cells (4, 5, 20, 47, 48).

### *Diffusible Nature of the AChR Dispersal Signal*

The ability of local signals such as nerve or beads to effect dispersal of preexisting AChR hot spots at a distance indicates that a component of the signal can propagate away from the site of synapse formation. To test whether this signal propagates by a diffusible process, we studied the rate of hot spot dispersal as a function of its distance from its closest bead-induced cluster by time-lapse recording. Fig. 2 *A* shows two hot spots on the same muscle cell undergoing dispersal as a result of HB-GAM bead application. The hot spot at position *a* at a distance of 20 μm away from its closest bead was dispersed much faster than the one at position *b*, which was 50 μm from its closest bead. Fig. 2 *B* shows the quantification of the dispersal process of a pair of hot spots in a bead-laden cell at 20 and 30 μm away from their nearest beads, respectively, as compared with a hot spot in a bead-free cell. Barring a small amount of photobleaching of the R-BTX image due to repeated recording, the hot spot remains stable in bead-free cells. In bead-treated cells, the hot spot dispersal can be fitted by an exponential decay curve. The time constant of the R-BTX fluorescence decay increases as a function of the distance between the hot spot and its nearest bead (Fig. 2 *B*).

The distance dependence was further studied in a population of cells. As shown in Fig. 2, *C* and *D*, a hot spot that lay immediately underneath a bead was dispersed within a few hours whereas one which was 190 μm away from a bead was relatively stable for hours. In this and subsequent experiments involving long-term, repeated observations of hot spots, it was necessary to reduce the excitation illumination to 1% of the normal lamp output with neutral density filters. However, despite a decrease in the signal-to-noise ratio of the images, the retention or the dispersal

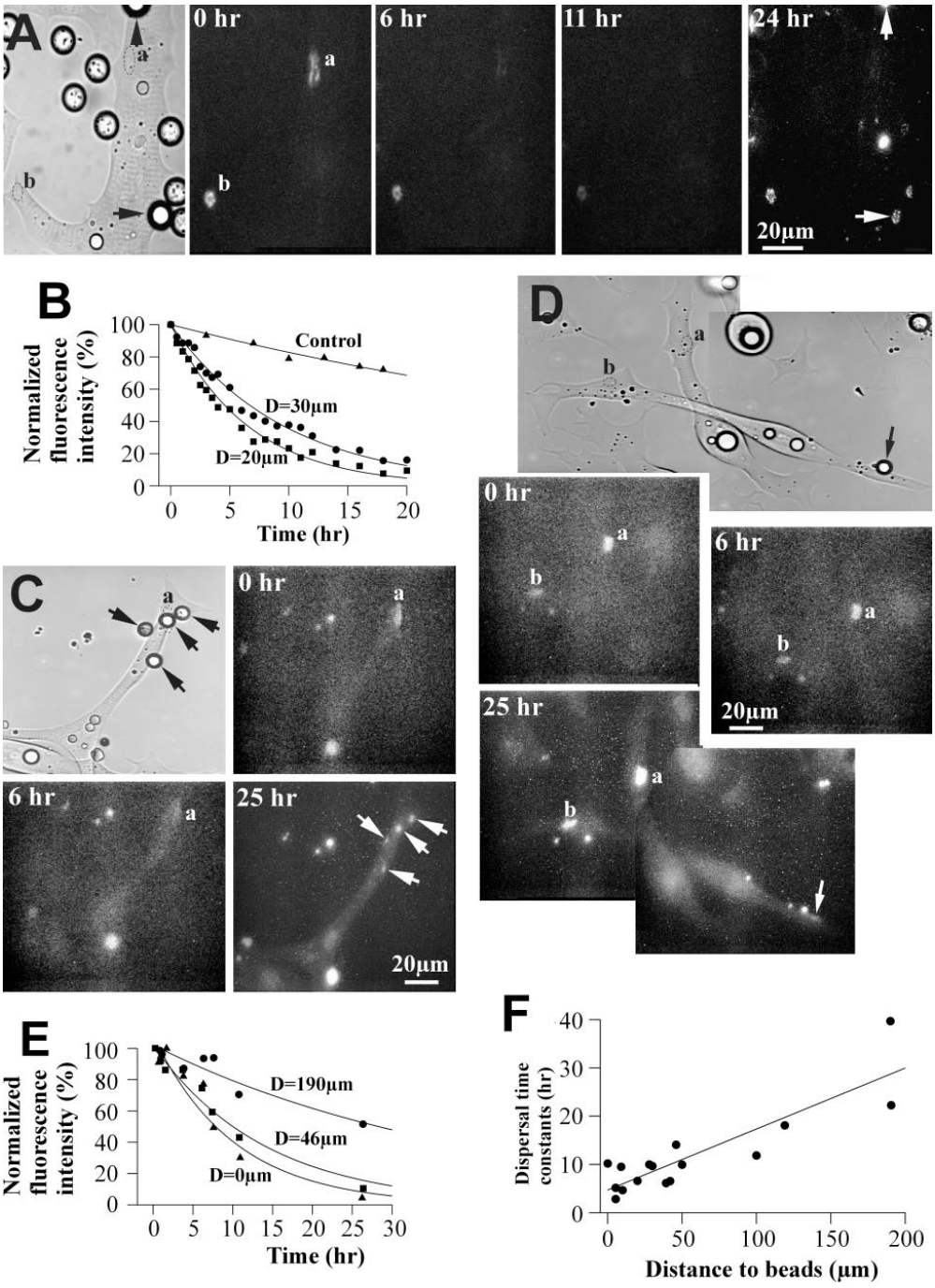


*Figure 2.* Dispersal of AChR hot spots as a function of distance to its nearest bead-induced new cluster. (*A*) Two hot spots at positions *a* and *b* underwent dispersal in response to bead-induced new cluster formation. The arrows point to two bead-induced clusters which were nearest to these two spots. Hot spot *a* is closer to a developing bead-induced cluster (*top arrow*) than hot spot *b* (*bottom arrow*). As the time sequence shows, *a* is dispersed at a much faster rate than *b*. The image at 24 h was contrast-enhanced to illustrate the bead-induced cluster (*arrows*). The same is true of the last time point in *C* and *D*. (*B*) Quantification of hot spot dispersal. Two hot spots on the same cell, one at a distance of 20 μm (*squares*) and the other at 30 μm (*circles*) away from its nearest bead-induced cluster, were recorded throughout the dispersal process. Triangles were measurements of a hot spot from a control cell not treated with beads. Points of each dispersal process can be well fitted with a simple exponential decay curve: $I(t) = I_0 e^{-t/\tau}$, where $I(t)$ and $I_0$ are intensities at time $t$ and 0, respectively, and $\tau$ is the time constant. This allows the calculation of the dispersal time constant. (*C*) A hot spot (*a*) immediately underneath a bead. It underwent dispersal quickly while new clusters formed under beads (*arrows*). (*D*) A hot spot (*b*) at a long distance (190 μm) from the closest bead. It showed very slow decrease in R-BTX fluorescence. Its intensity at 25 h was not much different from a control cluster (*a*). (*E*) Rate of dispersal of the two hot spots depicted in *C* ($D = 0$ mm) and *D* ($D = 190$ mm). The intermediate hot spot is from another cell. (*F*) Time constants of hot spot dispersal as a function of distance to nearest bead-induced AChR cluster. Each dot represents a single hot spot. Data were collected from 12 cells. A linear regression line is drawn through the data points. The correlation is highly significant with a correlation coefficient of 0.87 ($P < 0.0001$, Pearson product moment correlation test).

of hot spots were still clearly discernible. The dispersal of these two hot spots and another one at an intermediate distance was quantified in Fig. 2 *E*. From analyses like these, the time constants of 16 cells were determined and plotted against distance to the closest bead stimulus in Fig. 2 *F*. The correlation is highly significant with a correlation coefficient of 0.87 ($P < 0.0001$, Pearson product moment correlation test). Thus, the dispersal signal appears to emanate from the site of cluster formation via diffusion.

### *Innervation-induced Hot Spot Dispersal*

To understand whether innervation-induced hot spot dispersal is also mediated by a diffusible signal, time-lapse re-

cording was repeated in nerve–muscle cocultures. Unlike beads, the timing of nerve's contact with the muscle cell can not be determined accurately. In this experiment, neurons were seeded into muscle cultures and after an overnight incubation, hot spots on nerve-contacted muscle cells were followed. As shown in Fig. 3 *A*, a hot spot initially observed on the muscle cell (second panel) underwent dispersal after innervation and labeling was reduced to <10% the original intensity 24 h after the initial observation (third panel and its enhanced image in the fourth panel). Hot spots undergoing dispersal under the influence of nerve also maintained a great deal of structural integrity as shown in this (Fig. 3 *A*) and another (Fig. 3 *B*) example, despite the general decrease in receptor density.

By scoring the intensity of fluorescent BTX labeling at dispersing hot spots at the beginning of observation 24 h later, we measured their rate of dispersal as a function of distance to the nerve–muscle contact. As shown in Fig. 3 *C*, hot spot intensity at the end of the 24-h observation period was proportional to its distance from the nerve–muscle contact ($P < 0.05$). These results are consistent with those obtained from bead-induced hot spot dispersal and again implicate the role of a diffusible signal generated by innervation in this process.

### *The Effect of PTPase Inhibitors on AChR Cluster Dispersal and Formation*

Recent studies have shown that tyrosine phosphorylation plays a pivotal role in AChR clustering (5, 15, 59). Phosphotyrosine is one of the first markers to appear at developing AChR clusters and is also a constant feature of hot spots (5, 46). Its disappearance at hot spots undergoing dispersal suggests that the action of PTPases may be important for this process. To test this hypothesis, we first tested the effect of PTPase inhibitors on hot spot dispersal. PV is a potent inhibitor of PTPases (28, 51, 62). As shown in Fig. 4 *A*, at a concentration of 50 μM, PV inhibited the dispersal of hot spots induced by HB-GAM–coated beads. At this concentration, PV did not inhibit the formation of new clusters (Fig. 4 *A*). Thus, both preexisting hot spots and newly formed bead-induced clusters coexisted in these PV-treated cells. The dose-response curve of this inhibition is shown in Fig. 4 *F* which is fitted with the equation:

$$N = 1/(1 + k/[\mathrm{PV}])$$

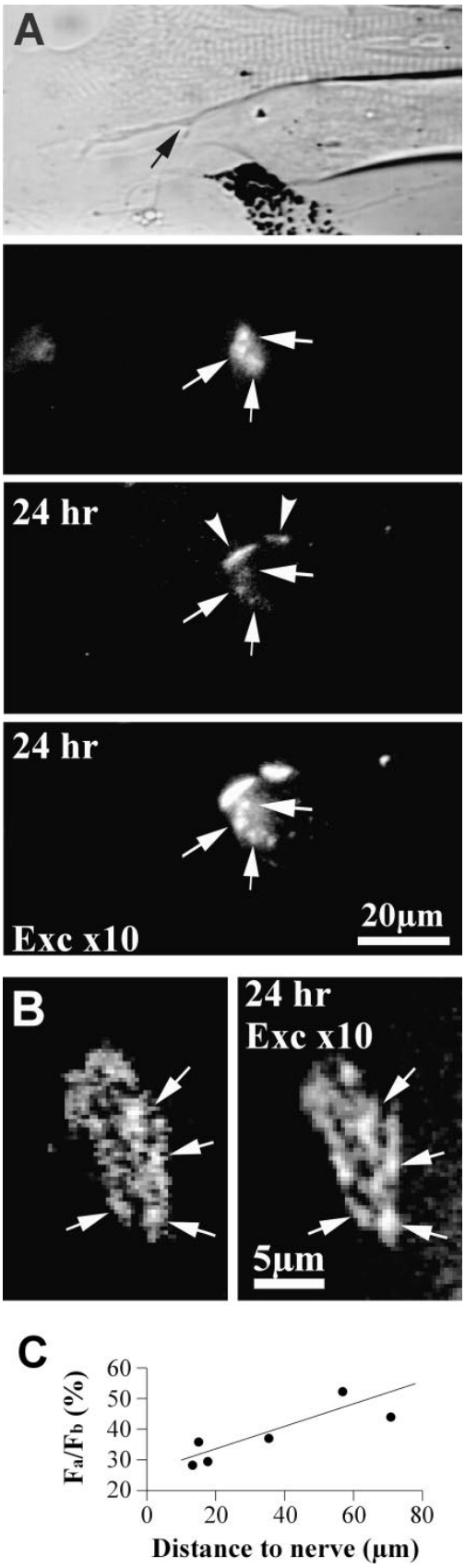


*Figure 3.* Innervation-induced hot spot dispersal. (*A*) Top panel: phase contrast; second panel: time zero of observation period (after overnight nerve–muscle coculture); third panel: 24 h after observation started; fourth panel: the same 24-h image visualized with a 10-fold increase in excitation light intensity. On this innervated muscle cell (bottom cell in the top panel), the motor nerve (*arrow*) induced the formation of an AChR cluster at nerve–muscle contact (*arrowheads* in the third panel, 24 h) and a preexisting hot spot (arrows in 2nd to 4th panels) was undergoing dispersal. After 24 h, features of the dispersing hot spot were still conserved as pointed out by arrows. (*B*) Fine structure of a hot spot undergoing nerve-induced dispersal. Well-preserved structural features are pointed out by arrows. The 24 h image was taken with 10× excitation. (*C*) Change in hot spot intensity as a function of its distance to nerve–muscle contact. $F_a$ and $F_b$, fluorescence intensity of hot spots (after background subtraction) at 0 and 24 h of observation period. A linear regression line is drawn through the data points. The correlation is significant with a correlation coefficient of 0.84 ($P < 0.05$, Pearson product moment correlation test).

where $N$ is the percentage of cells with hot spots at a given PV concentration, [$PV$] is the PV concentration and $k$ is the half-inhibition concentration.

From this equation the half-inhibition concentration for hot spot dispersal was calculated to be 18 μM. At higher concentrations, PV did inhibit the formation of AChR clusters. By scoring AChR clusters at bead-muscle contacts, the effect of PV on this process was also studied as shown in Fig. 4 *F*. The half-inhibition concentration of cluster formation was determined to be 90 μM, which is much higher than the concentration for inhibiting hot spot dispersal.

In addition to beads, we also examined cluster dispersal induced by innervation. Muscle cultures were seeded with neurons and after an overnight coculture to establish nerve–muscle contacts, PV (75 μM) was introduced and its effect on hot spot dispersal in innervated cells was studied 24 h later. Similar to the situation of bead-induced clustering, PV did not prevent cluster formation at nerve–muscle contacts at low concentrations, but it significantly inhibited the dispersal of hot spots in nerve–muscle cocultures ($P < 0.001$, number of nerve–muscle pairs scored: 22 in the control group and 18 in PV treatment group).

In addition to PV, we also tested effect of PAO, another PTPase inhibitor (22). As shown in Fig. 4 *G*, PAO at concentrations ranging from 1–10 nM also inhibited bead-induced hot spot dispersal. The dose dependence of this inhibition is shown in Fig. 4 *H*. The half inhibitory concentration for cluster dispersal is 2.4 nM for PAO. At higher concentrations, PAO also inhibited bead-induced cluster formation. However, the half-inhibition concentration is 8.5 nM for the latter process. Taken together, these results suggest a role of PTPase in hot spot dispersal.

At intermediate PTPase inhibitor concentrations, an interesting effect on AChR cluster formation was observed. Without the inhibitor, AChRs are clustered discretely at bead–muscle contacts (Fig. 4 *B*, *R-BTX*) or at nerve–muscle contacts (Fig. 4 *D*). The boundary of R-BTX labeled area at these sites is well defined. PV (50 μM) or PAO (10 nM) caused a blurring of this sharp boundary in such a way that AChRs were no longer confined to bead or nerve contact sites (Fig. 4 *C*, *R-BTX*, *E* and *G*). Punctate AChR aggregates appeared scattered over a larger area surrounding the site of stimulation. These data are consistent with the idea that both tyrosine kinase and phosphatase are activated by synaptic stimulus and the spatial spread of the kinase signal is checked by the PTPase activity. When the latter is suppressed, tyrosine phosphorylation can not be strictly contained within confines of the stimulus and thus can spread. Consistent with this hypothesis is the observation that the highly localized AChR clustering is normally paralleled by equally discrete phosphotyrosine labeling (Fig. 4 *B*, *PY*). In PV-treated cells, however, the phosphotyrosine labeling was spread over a much broader area (Fig. 4 *C*, *PY*). Thus, coordinated activation of tyrosine kinase and PTPase is needed for discrete AChR clustering at the site of synaptic induction.

### *Dispersal of Hot Spots by Exogenous PTPase*

To provide direct evidence on the involvement of PTPase in hot spot disassembly, we studied the effect of exogenously introduced PTPase in cultured muscle cells. A 51-kD peptide that contains the catalytic domain of the PTPase from *Yersinia enterocolitica* (61) was introduced into cultured muscle cells by the patch–clamp method. Fluorescein-labeled dextran was cointroduced as a marker. Before loading, muscle cells were prelabeled with R-BTX. Hot spots on test cells were mapped before loading and followed for up to 30 h after loading. The loading procedure alone had no effect on the stability of hot spots as shown in Fig. 5 *B*. In this example, the muscle cell was loaded with FITC-dextran alone. Hot spots in cells loaded with dextran alone remained stable 24 h after the treatment, similar to control, unperturbed cells (Fig. 5 *A*, *arrows*). On the other hand, hot spots on cells loaded with both PTPase and dextran were dispersed. As shown in the example in Fig. 5 A (bifurcated arrowhead), the hot spot was completely dispersed 24 h after intracellular introduction of *Yersinia* PTPase. Results of several experiments summarized in Fig. 5 *D* clearly show that PTPase loading directly results in hot spot dispersal in the absence of AChR clustering stimuli such as beads or nerve. Furthermore, the time course of PTPase-effected dispersal is similar to that induced by bead stimulation (Fig. 2 *B*).

The specificity of the effect on hot spot dispersal by exogenous PTPase was further examined through the use of the PTPase inhibitor PV. As shown in Fig. 5 *C*, *PV*, at a concentration of 70 μM completely blocked the effect of *Yersinia* PTPase in causing hot spot dispersal. At this concentration, the activity of both endogenous and exogenous PTPase is presumably blocked.

These PTPase injection experiments were repeated a number of times using different batches of muscle culture and results are summarized in Fig. 5 *E*. In each category, the ratio of mean hot spot fluorescence intensity before and 24 h after injection was calculated. In control cells loaded with FITC-dextran only, there was no reduction in hot spot intensity. PTPase injection resulted in hot spot dispersal as indicated by the reduction in mean hot spot intensity to 20% of the control value ($P < 0.001$). In the presence of PV, there was no reduction in hot spot intensity after PTPase injection. Thus, these results further support the involvement of PTPase in AChR cluster dispersal.

## *Discussion*

In this study, we presented two lines of evidence that implicate a role of PTPase in the dispersal of AChR clusters in skeletal muscle cells. First, the dispersal of preexisting AChR hot spots induced by the stimulus that induces the formation of new clusters can be prevented by PTPase inhibitors such as PV and PAO. Second, an exogenous PTPase introduced intracellularly causes hot spot dispersal independent of new cluster formation. In addition, the abolishment of the exogenous PTPase-induced hot spot dispersal by PV treatment further confirms the specific activities of both PV and *Yersinia* PTPase. Our observation that PTPase inhibitors cause a scattering effect of AChR clustering has also revealed a role of PTPase in the assembly of this postsynaptic specialization. These data thus suggest that PTPase activation is a critical step in postsynaptic development at the NMJ.

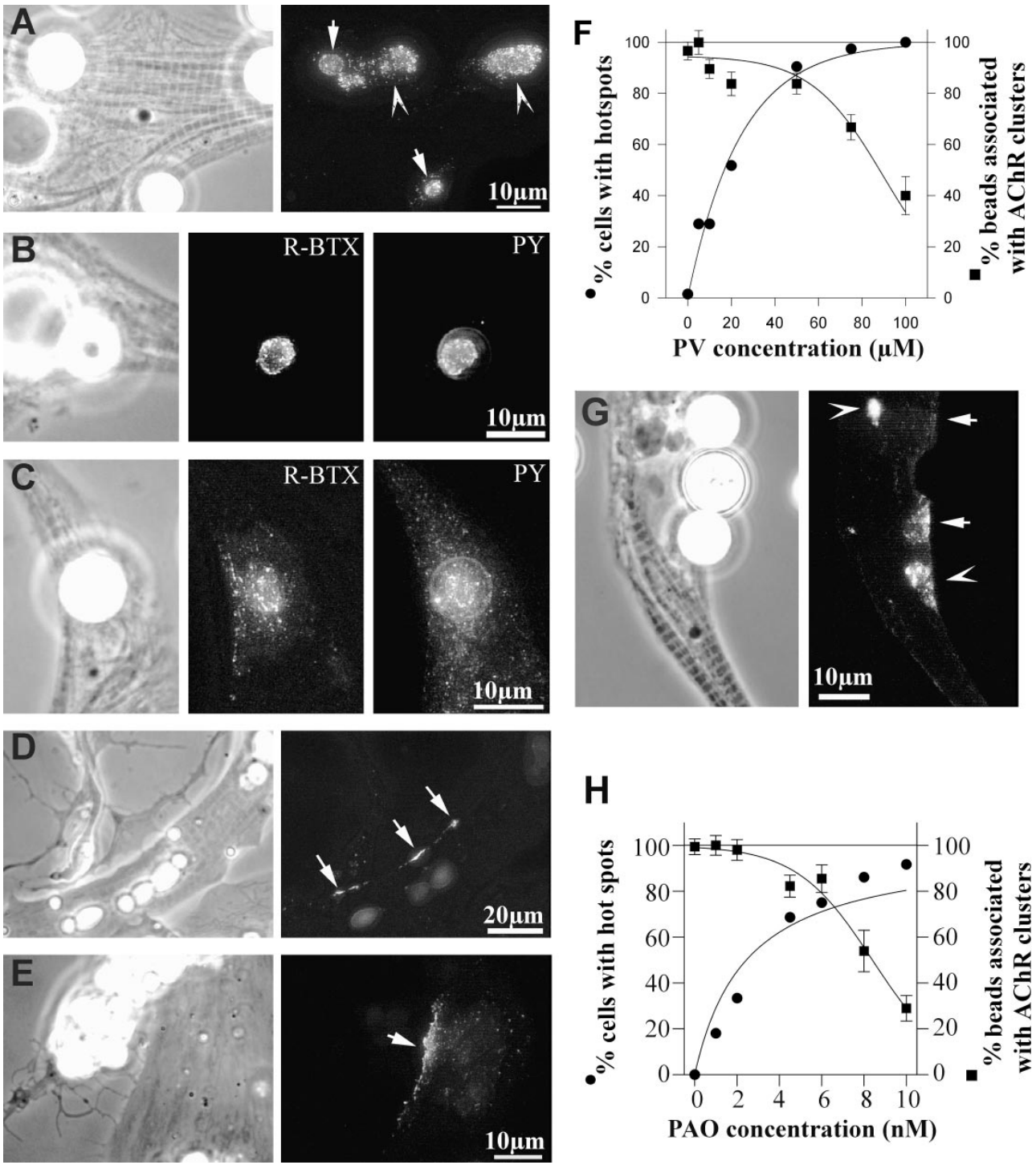


*Figure 4.* Effect of PTPase inhibitors on AChR cluster dispersal and formation. (*A*) PV at 50 μM prevented the dispersal of hot spots (*two-tailed arrowheads*) on a bead-stimulated muscle cell. This image was taken 24 h after bead treatment. Both bead-induced clusters (*arrows*) and hot spots coexisted. (*B* and *C*) Effect of PV on the formation of bead-induced clusters. AChRs, as well as phosphotyrosine labeling, were discretely concentrated at the site of bead stimulation in the control (*B*). PV (50 μM) caused AChR and phosphotyrosine cluster to assume a more scattered appearance (*C*). Small punctate aggregates were seen over a broad area around the bead. (*D* and *E*) PV effect on NMJ formation. AChR clusters form discretely at nerve–muscle contacts in the control (*D*). Clusters appeared more scattered in the presence of PV at 50 μM (*E*). Nerve–muscle contacts are shown in phase contrast on the left of each example. (*F*) Dose dependence of the PV effect on bead-induced cluster formation and dispersal. At 50 μM, PV nearly abolished the dispersal without significantly affecting the cluster formation. At higher concentrations, discrete clusters failed to form in the presence of pervanadate. The equation for fitting the hot spot data is described in the text. The data on bead-induced clustering were fitted with the equation: $N = N_{max}/(1 + \exp[0.06\{[PV] - 90\}])$, where $N_{max}$ and $N$ are the percentage of beads with AChR clusters at 0 and a given PV concentration, respectively, and [PV] is the PV concentration. The curves are normalized to the control. (*G*) Effect of PAO (10 nM) on preserving hot

### *The Formation and Dispersal of Hot Spots*

Hot spots, defined as AChR clusters not associated with the motor terminal, are a salient feature of cultured skeletal muscle cells (2, 17, 56). Although not observed in normally innervated muscle in vivo, they also develop if innervation is disrupted and in denervated muscle (13, 33, 53). A recent study has also shown that aneural AChR clusters can develop in agrin-deficient mice (23). Interestingly, when agrin is expressed in the extrajunctional area of an innervated muscle, AChR clusters are also induced (30, 38). These aneural AChR clusters, both in vitro and in vivo, generally have a full complement of postsynaptic specializations, including AChRs, junctional folds, specialized basal lamina, acetylcholinesterase and postsynaptic proteins (38, 42, 60). Their induction by the neuronal isoform of agrin (38) suggests that they are induced by the same kind of signaling mechanism involved in the formation of the postsynaptic membrane. However, the formation of these clusters in aneural muscle cells in vivo and in vitro suggests that they can also form in response to nonneuronally derived signals. Our work on the induction of aneural AChR clusters with beads coated with heparin-binding growth factors (43, 44) suggests the involvement in their formation of peptide growth factors bound to the heparan-sulfate proteoglycans in the muscle's basement membrane.

Once formed, hot spots are stable in the absence of new synaptogenic stimulation (39). As previously shown, their dispersal can be induced by innervation, beads or agrin treatment (14, 34, 39, 41). This study has shown that the disassembly involves the removal of a key link between AChRs and the cytoskeletal complex underlying the hot spot without the dismantling of the entire complex. This is echoed by the step-by-step development of the postsynaptic cytoskeleton with respect to AChR cluster formation as we previously reported (4, 47). Using bead-induced AChR clustering as a model, we found that although receptor clustering can be observed within a few hours, not all postsynaptic specializations follow this time course. The assembly of the F-actin and the appearance of phosphotyrosine labeling precede the clustering of AChRs and rapsyn appears with the same time course as AChRs (5, 48–50). Thus, the interaction among AChR, rapsyn, and F-actin induced by the synaptogenic stimulus may be a key event in the formation of the postsynaptic receptor cluster and its disruption may underlie its dispersal. On the other hand, specializations such as membrane infoldings, dystrophin, and FAK localization, are assembled at a much slower time course. In fact, some of these proteins within the postsynaptic protein complex are probably not directly associated with the AChR domain but with the postsynaptic folds (9, 47). This may account for their persistence after AChR dispersal. The essential role of rapsyn has been demonstrated in gene knockout studies (24). Mice with null rapsyn expression have no AChR clusters despite the presence of NMJs. Thus, rapsyn may mediate the attachment of AChRs to the postsynaptic cytoskeleton. A recent study has suggested the presence of a transmembrane linker that interacts with rapsyn and a scaffold containing the receptor tyrosine kinase MuSK (3). It is tempting to speculate that this interaction may become inhibited upon cluster dispersal.

### *The Involvement of Tyrosine Kinase and Phosphatase in AChR Clustering*

The formation of AChR cluster discretely at the site of innervation indicates that its signaling is highly localized. Recent studies have shown that the activation of the receptor tyrosine kinase MuSK is a key component in this signaling (15, 21, 25, 57). Mice with targeted deletion of the MuSK gene show disrupted NMJ formation with no AChR clustering (15). In addition to activating a local signaling system, the induction of hot spot dispersal clearly shows that innervation also exerts a global influence on the muscle cell. The nature of this global signal was hitherto unknown. Results from this study have clearly shown that the rate of hot spot dispersal is inversely related to its distance from the site of synaptogenic stimulation. Thus, the dispersal signal emanating from the clustering signal propagates to the target site by a diffusion-mediated mechanism.

At present, the molecular nature of the PTPase-sensitive link that is important for the stability of the AChR cluster in not known. One possible candidate is the AChR itself as it is a substrate for tyrosine phosphorylation (59). Although previous studies suggested that tyrosine phosphorylation of AChR, in particular the β subunit, is important for their clustering (59), recent results have shown that AChRs with all three cytoplasmic tyrosine residues on the β subunit mutated are still capable of clustering in response to agrin in myotubes (Meyer, G., and B.G. Wallace. 1998. Keystone Symposia on Synapse Formation and Function. Abstract no. 306). We recently found that cross-linking AChRs by biotinylated α-bungarotoxin followed by streptavidin inhibits the formation of AChR but not PY clusters induced by beads in *Xenopus* muscle cells. Furthermore, AChR hot spots in these treated cells remain while their associated PY undergoes dispersal in response to beads (our unpublished results). These results are consistent with the notion that AChR's tyrosine phosphorylation is not directly correlated with its clustering or dispersal. Thus, the target for the PTPase action may not be the AChR and seems to involve other molecule(s) yet to be identified.

As our current work shows, PTPases activation is a component of this global signaling. At high concentration, PTPase inhibitors also block the formation of AChR clusters. This result is consistent with previously published result on the inhibition of agrin-induced AChR clustering by

spots. Both new clusters induced by beads (*arrows*) and preexisting hot spots (*two-tailed arrowheads*) coexist. Bead-induced clusters also assume a diffuse appearance under PAO treatment. (*H*) Dose-response of PAO effects on AChR formation and dispersal. The equation for fitting the hot spot data is the same as that for PV (*F*). The data on bead-induced clustering were fitted with the equation: $N = N_{max}/(1 + \exp[0.56\{[PAO] - 8.395\}])$.

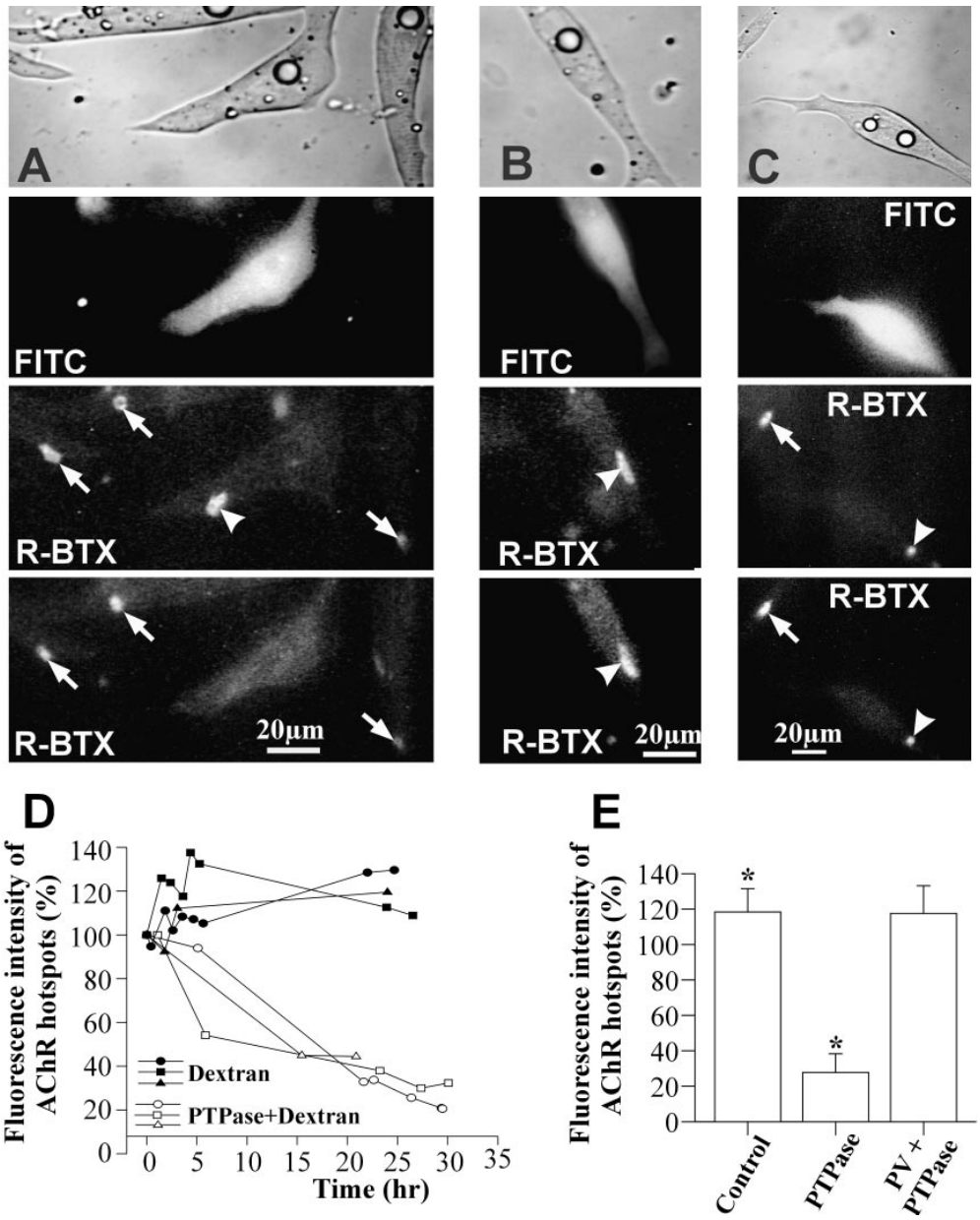


*Figure 5.* Effect of PTPase injection on cluster dispersal. (*A*) PTPase and FITC-dextran injection. The cell in the middle was injected with *Yersinia* PTPase together with FITC-dextran. Before injection, all cells in the field had AChR hot spots (*arrows* and *two-tailed arrowhead* in the top R-BTX panel). 24 h after PTPase injection (bottom R-BTX panel), the hot spot disappeared on the PTPase-injected cell, while they persisted on uninjected cells (*arrows*). (*B*) Control FITC-dextran injection. The hot spot on dextran-injected cell was unaffected 24 h after injection. (*C*) PTPase and FITC-dextran injection in the presence of PV (75 μM). The hot spot on the injected cell remained intact (*two-tailed arrowheads*). (*D*) Time course of hot spot dispersal resulting from direct PTPase injection compared with control cells. (*E*) Ratio of mean fluorescence intensity of AChR hot spots at 24 h after injection over its original state. Control (FITC-dextran), $n$ (number of cells) = 11; PTPase, $n$ = 11; PV+PTPase, $n$ = 3. The difference between control and PTPase is highly statistically significant ($P < 0.001$).

PV (37, 58). In that study, a decrease in the mobility and detergent extractability of AChRs was found to result from PV treatment. However, in the current study, we observed that at low concentration, PTPase inhibitors do not prevent nerve-induced or bead-induced AChR clustering. Thus, the mobility of AChRs must remain largely intact under such condition.

The blurring of the boundary of AChR clusters as a result of PTPase inhibition by PV treatment also suggests a novel role of this enzyme in the assembly of postsynaptic specialization. The discreteness of the AChR clustering mechanism is needed to allow the receptors to achieve high density at the postsynaptic membrane. Results from this study indicate that this is accomplished through orchestrated activities of tyrosine kinase and PTPase. The local kinase activation is undoubtedly a prerequisite for postsynaptic differentiation. However, without the participation of PTPase, the signal tends to diffuse to surrounding areas, as evidenced by the spread of both phosphotyrosine and AChR labeling. In this sense, the PTPase serves as a sink to regulate the intensity of tyrosine phosphorylation emanating from the kinase source at the site of innervation. Thus, by turning on both a source (RTK activation) and a sink (PTPase activation) of tyrosine phosphorylation, a steep gradient of signaling events centered around the site of nerve–muscle or nerve–bead contact can be achieved.

A model depicting the roles of tyrosine kinase and phosphatase in AChR clustering is shown in Fig. 6. In this model, the state of individual AChRs, either diffusely distributed or clustered, is depicted as a function of the combined action of tyrosine kinase and phosphatase. In the quiescent state (Fig. 6 *A*), AChRs are diffusely distributed except at hot spots. A basal level of PTPase activity suppresses the kinase activity except at the hot spot where there is an elevation of phosphotyrosine (5). The basal level of

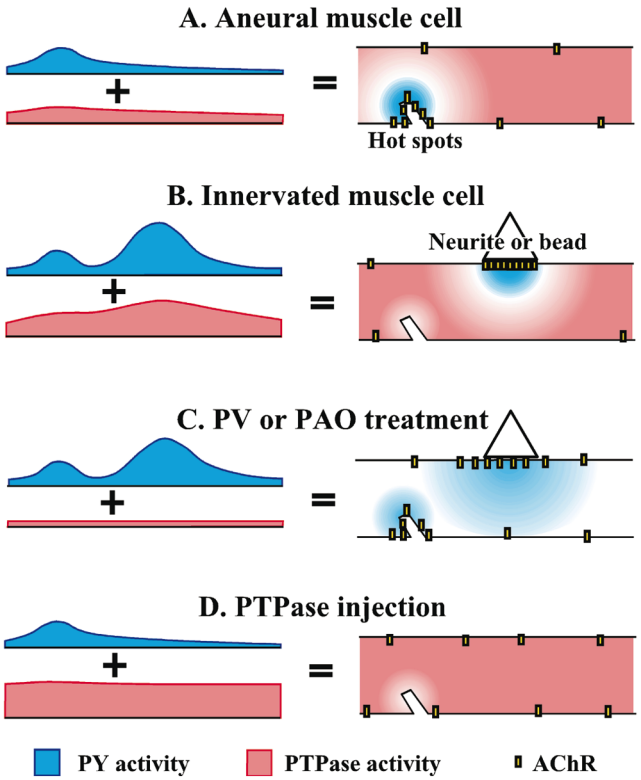


*Figure 6.* A model for PTPase in AChR cluster formation and dispersal. (*A*) In the absence of innervation, AChRs form clusters spontaneously. These sites are usually associated with phosphotyrosine concentration. The left side shows the level of either kinase activity (*blue*) or PTPase activity (*red*). The right side shows a lateral profile of the muscle cell. (*B*) Innervation or growth factor–coated bead locally activates receptor tyrosine kinases at the site of stimulation and also raises the PTPase activity in a diffuse manner. This results in AChR clustering discretely at the site of stimulation and the dispersal of AChR hot spots distally. (*C*) Inhibition of PTPase activity by pervanadate causes the diffusion of the kinase signal, resulting in more diffuse clustering process at the site of stimulation, and the retention of AChR hot spots. (*D*) Injection of exogenous PTPase raises the activity of this enzyme throughout the muscle cell and causes hot spot dispersal in the absence of synaptogenic stimulus.

PTPase suppresses AChR clustering in the rest of the cell. Upon innervation (or the presentation of growth factor–coated beads), both a receptor tyrosine kinase and a PTPase are activated, first at the site of nerve (or bead) contact (Fig. 6 *B*). The sphere of influence of the kinase is restricted by PTPase, resulting in discrete AChR clustering. The diffusion of PTPase activity also results in dephosphorylation at hot spots, rendering their dispersal. When PTPase is suppressed by an inhibitor such as PV (Fig. 6 *C*), the kinase activity stimulated by the presynaptic signal is unchecked, resulting in the diffusion of the kinase signal and a scattering of the clustering process as seen in Fig. 4 (*C* and *E*). The basal level of tyrosine phosphorylation at the hot spot is retained, thus leaving it intact. The intracellular introduction of an exogenous PTPase such as *Yersinia* PTPase, causes dephosphorylation at the hot spot and its dispersal (Fig. 6 *D*).

A similar principle may apply to synaptogenesis in the central nervous system. Since a single soma or dendrite of a central neuron often accommodates a large number of synapses with distinct characteristics such as excitatory versus inhibitory or different receptor subtypes (7, 16), a mechanism to demarcate receptor patches underneath individual presynaptic terminals is essential. The regulation of signaling by coupling a source with a sink depicted here may also be necessary for the demarcation process on a central neuron, although the signal used in that process may be different and considerably more complex than the monosynaptic situation of the NMJ.

### *The Nature of the PTPase*

The diffusible nature of the cluster-dispersing signal suggests that the PTPase of interest is diffusible, or it is activated by a diffusible second messenger such as calcium or intermediates generated in the kinase cascade. Since a PTPase introduced into the cytoplasm can reproduce the cluster dispersal process with approximately the same time course as that produced by synaptogenic stimulation, we think that a cytoplasmic PTPase is most likely involved. The skeletal muscle expresses a number of PTPases, including SHP2 (also known as SH-PTP2, PTP1D) which contains two Src homology 2 (SH2) domains (1, 35, 36). This PTPase interacts with signal transduction proteins including receptor tyrosine kinases and nicotinic AChRs via its SH2 domain (36, 40). Thus, this PTPase is an attractive candidate for RTK-activated cluster dispersal mechanisms. Conceivably, the activation of RTKs at the site of nerve–muscle or bead–muscle contacts leads to the activation of a PTPase pathway which, by serving as a diffusible signal itself or by triggering the generation of downstream diffusible messengers, causes the destabilization of AChR hot spots.

The removal of redundant AChR clusters from the surface of skeletal muscle fibers is an integral part of NMJ development. During the elimination of polyneuronal innervation, AChR clusters underneath retracting nerve terminals are removed as a result of synaptic competition (10, 11). Recent studies have shown that the disassembly of AChR clusters actually precedes the retraction of the redundant nerve terminal (6). Thus, the "winning" nerve terminal may induce the formation of a diffusible messenger to effect the dispersal of neighboring AChR clusters, which is followed by the retraction of redundant terminals (29). This process may be analogous to the dispersal of hot spots discussed here, except for the fact that synaptic competition is activity dependent. It is possible that synaptic activity can further promote PTPase effect in eliminating redundant AChR clusters during synaptic competition.

We thank Drs. Stan Froehner, Teiji Khurana, Tom Parsons, Rick Rotundo, and Heikki Rauvala for reagents used in this study.

This work was supported by National Institutes of Health grant NS-23583 and the Muscular Dystrophy Association.

Received for publication 20 November 1997 and in revised form 29 May 1998.

#### *References*

1. Ahmad, S., D. Banville, Z. Zhao, E.H. Fischer, and S.-H. Shen. 1993. A widely expressed human protein-tyrosine phosphatase containing *src* homology 2 domains. *Proc. Natl. Acad. Sci. USA*. 90:2197–2201.
2. Anderson, M.J., and M.W. Cohen. 1977. Nerve-induced and spontaneous redistribution of acetylcholine receptors on cultured muscle cells. *J. Physiol. (Lond.)*. 268:757–773.

3. Apel, E.D., D.J. Glass, L.M. Moscoso, G.D. Yancopoulos, and J.R. Sanes. 1997. Rapsyn is required for MuSK signaling and recruits synaptic components to a MuSK-containing scaffold. *Neuron*. 18:623–635.
4. Baker, L.P., D.F. Daggett, and H.B. Peng. 1994. Concentration of pp125 focal adhesion kinase (FAK) at the myotendinous junction. *J. Cell Sci.* 107: 1485–1497.
5. Baker, L.P., and H.B. Peng. 1993. Tyrosine phosphorylation and acetylcholine receptor cluster formation in cultured *Xenopus* muscle cells. *J. Cell Biol.* 120:185–195.
6. Balice-Gordon, R.J., and J.W. Lichtman. 1994. Long-term synapse loss induced by focal blockade of postsynaptic receptors. *Nature*. 372:519–524.
7. Bechade, C., and A. Triller. 1996. The distribution of glycine receptors and interactions with the cytoskeleton. *Sem. Cell Dev. Biol.* 7:717–724.
8. Bloch, R.J., and D.W. Pumplin. 1988. Molecular events in synaptogenesis: nerve-muscle adhesion and postsynaptic differentiation. *Am. J. Physiol.* 254:C345–C364.
9. Chen, Q., R. Sealock, and H.B. Peng. 1990. A protein homologous to the *Torpedo* postsynaptic 58K protein is present at the myotendinous junction. *J. Cell Biol.* 110:2061–2071.
10. Colman, H., and J.W. Lichtman. 1993. Interactions between nerve and muscle: synapse elimination at the developing neuromuscular junction. *Dev. Biol.* 156:1–10.
11. Colman, H., J. Nabekura, and J.W. Lichtman. 1997. Alterations in synaptic strength preceding axon withdrawal. *Science*. 275:356–361.
12. Craig, A.M., C.D. Blackstone, R.L. Huganir, and G. Banker. 1994. Selective clustering of glutamate and gamma-aminobutyric acid receptors opposite terminals releasing the corresponding neurotransmitters. *Proc. Natl. Acad. Sci. USA*. 91:12373–12377.
13. Creazzo, T.L., and G.S. Sohal. 1983. Neural control of embryonic acetylcholine receptor and skeletal muscle. *Cell Tissue Res.* 228:1–12.
14. Daggett, D.F., D. Stone, H.B. Peng, and K. Nikolics. 1996. Full-length agrin isoform activities and binding site distributions on cultured *Xenopus* muscle cells. *Mol. Cell. Neurosci.* 7:75–88.
15. DeChiara, T.M., D.C. Bowen, D.M. Valenzuela, M.V. Simmons, W.T. Poueymirou, S. Thomas, E. Kinetz, D.L. Compton, E. Rojas, J.S. Park, et al. 1996. The receptor tyrosine kinase MuSK is required for neuromuscular junction formation in vivo. *Cell*. 85:501–512.
16. Farb, C.R., C. Aoki, and J.E. Ledoux. 1995. Differential localization of NMDA and AMPA receptor subunits in the lateral and basal nuclei of the amygdala: a light and electron microscopic study. *J. Comp. Neurol.* 362:86–108.
17. Fischbach, G.D., and S.A. Cohen. 1973. The distribution of acetylcholine sensitivity over uninnervated and innervated muscle fibers grown in cell culture. *Dev. Biol.* 31:147–162.
18. Froehner, S.C. 1991. The submembrane machinery for nicotinic acetylcholine receptor clustering. *J. Cell Biol.* 114:1–7.
19. Froehner, S.C. 1993. Regulation of ion channel distribution at synapses. *Annu. Rev. Neurosci.* 16:347–368.
20. Froehner, S.C., A.A. Murnane, M. Tobler, H.B. Peng, and R. Sealock. 1987. A postsynaptic $M_r$ 58,000 (58K) protein concentrated at acetylcholine receptor-rich sites in *Torpedo* electroplaques and skeletal muscle. *J. Cell Biol.* 104:1633–1646.
21. Ganju, P., E. Walls, J. Brennan, and A.D. Reith. 1995. Cloning and developmental expression of Nsk2, a novel receptor tyrosine kinase implicated in skeletal myogenesis. *Oncogene*. 11:281–290.
22. Garcia-Morales, P., Y. Minami, E. Luong, R.D. Klausner, and L.E. Samelson. 1990. Tyrosine phosphorylation in T cells is regulated by phosphatase activity: studies with phenylarsine oxide. *Proc. Natl. Acad. Sci. USA*. 87:9255–9259.
23. Gautam, M., P.G. Noakes, L. Moscoso, F. Rupp, R.H. Scheller, J.P. Merlie, and J.R. Sanes. 1996. Defective neuromuscular synaptogenesis in agrin-deficient mutant mice. *Cell*. 85:525–535.
24. Gautam, M., P.G. Noakes, J. Mudd, M. Nichol, G.C. Chu, J.R. Sanes, and J.P. Merlie. 1995. Failure of postsynaptic specialization to develop at neuromuscular junctions of rapsyn-deficient mice. *Nature*. 377:232–236.
25. Glass, D.J., D.C. Bowen, T.N. Stitt, C. Radziejewski, J. Bruno, T.E. Ryan, D.R. Gies, S. Shah, K. Mattsson, S.J. Burden, et al. 1996. Agrin acts via a MuSK receptor complex. *Cell*. 85:513–523.
26. Hall, Z.W., and J.R. Sanes. 1993. Synaptic structure and development: the neuromuscular junction. *Neuron*. 10(Suppl.):99–121.
27. Hamill, O.P., A. Marty, E. Neher, B. Sakmann, and F.J. Sigworth. 1981. Improved patch-clamp techniques for high-resolution current recording from cells and cell-free membrane patches. *Pflugers Arch.* 391:85–100.
28. Heffetz, D., I. Bushkin, R. Dror, and Y. Zick. 1990. The insulinomimetic agents $H_2O_2$ and vanadate stimulate protein tyrosine phosphorylation in intact cells. *J. Biol. Chem.* 265:2896–2902.
29. Jennings, C. 1994. Death of a synapse. *Nature*. 372:498–499.
30. Jones, G., T. Meier, M. Lichtsteiner, V. Witzemann, B. Sakmann, and H.R. Brenner. 1997. Induction by agrin of ectopic and functional postsynaptic-like membrane in innervated muscle. *Proc. Natl. Acad. Sci. USA*. 94:2654–2659.
31. Kidokoro, Y., and B. Brass. 1985. Redistribution of acetylcholine receptors during neuromuscular junction formation in *Xenopus* cultures. *J. Physiol.* 80:212–220.
32. Kirsch, J., and H. Betz. 1995. The postsynaptic localization of the glycine receptor-associated protein gephyrin is regulated by the cytoskeleton. *J. Neurosci.* 15:4148–4156.
33. Ko, P.K., M.J. Anderson, and M.W. Cohen. 1977. Denervated skeletal muscle fibers develop discrete patches of high acetylcholine receptor density. *Science*. 196:540–542.
34. Kuromi, H., and Y. Kidokoro. 1984. Nerve disperses preexisting acetylcholine receptor clusters prior to induction of receptor. *Dev. Biol.* 103:53–61.
35. Mei, L., C.A. Doherty, and R.L. Huganir. 1994. RNA splicing regulates the activity of a SH2 domain-containing protein tyrosine phosphatase. *J. Biol. Chem.* 269:12254–12262.
36. Mei, L., and J. Si. 1995. Tyrosine phosphorylation and synapse formation at the neuromuscular junction. *Life Sciences.* 57:1459–1466.
37. Meier, T., G.M. Perez, and B.G. Wallace. 1995. Immobilization of nicotinic acetylcholine receptors in mouse C2 myotubes by agrin-induced protein tyrosine phosphorylation. *J. Cell Biol.* 131:441–451.
38. Meier, T., D.M. Hauser, M. Chiquet, L. Landmann, M.A. Ruegg, and H.R. Brenner. 1997. Neural agrin induces ectopic postsynaptic specializations in innervated muscle fibers. *J. Neurosci.* 17:6534–6544.
39. Moody-Corbett, F., and M.W. Cohen. 1982. Influence of nerve on the formation and survival of acetylcholine receptor and cholinesterase patches on embryonic Xenopus muscle cells in culture. *J. Neurosci.* 2:633–646.
40. Neel, B.G., and N.K. Tonks. 1997. Protein tyrosine phosphatases in signal transduction. *Curr. Opin. Cell Biol.* 9:193–204.
41. Peng, H.B. 1986. Elimination of preexistent acetylcholine receptor clusters induced by the formation of new clusters in the absence of nerve. *J. Neurosci.* 6:581–589.
42. Peng, H.B. 1987. Development of the neuromuscular junction in tissue culture. *CRC Crit. Rev. Anat. Sci.* 1:91–131.
43. Peng, H.B., A.A. Ali, Z. Dai, D.F. Daggett, E. Raulo, and H. Rauvala. 1995. The role of heparin-binding growth-associated molecule (HB-GAM) in the postsynaptic induction in cultured muscle cells. *J. Neurosci.* 15:3027–3038.
44. Peng, H.B., L.P. Baker, and Q. Chen. 1991. Induction of synaptic development in cultured muscle cells by basic fibroblast growth factor. *Neuron*. 6:237–246.
45. Peng, H.B., L.P. Baker, and Q. Chen. 1991. Tissue culture of *Xenopus* neurons and muscle cells as a model for studying synaptic induction. In *Xenopus laevis*: practical uses in cell and molecular biology. *Methods Cell Biol.* 36:511–526.
46. Peng, H.B., L.P. Baker, and Z. Dai. 1993. A role of tyrosine phosphorylation in the formation of acetylcholine receptor clusters induced by electric fields in cultured *Xenopus* muscle cells. *J. Cell Biol.* 120:197–204.
47. Peng, H.B., and Q. Chen. 1992. Induction of dystrophin localization in cultured *Xenopus* muscle cells by latex beads. *J. Cell Sci.* 103:551–563.
48. Peng, H.B., and S.C. Froehner. 1985. Association of the postsynaptic 43K protein with newly formed acetylcholine receptor clusters. *J. Cell Biol.* 100:1698–1705.
49. Peng, H.B., and K.A. Phelan. 1984. Early cytoplasmic specialization at the presumptive acetylcholine receptor cluster: a meshwork of thin filaments. *J. Cell Biol.* 99:344–349.
50. Peng, H.B., H. Xie, and Z. Dai. 1997. The association of cortactin with developing neuromuscular specializations. *J. Neurocytol.* 26:637–650.
51. Pumiglia, K.M., L.F. Lau, C.K. Huang, S. Burroughs, and M.B. Feinstein. 1992. Activation of signal transduction in platelets by the tyrosine phosphatase inhibitor pervanadate (vanadyl hydroperoxide). *Biochem. J.* 286:441–449.
52. Sheng, M. 1997. Excitatory synapses—glutamate receptors put in their place. *Nature*. 386:221–223.
53. Sohal, G.S. 1988. Development of postsynaptic-like specializations of the neuromuscular synapse in the absence of motor nerve. *Int. J. Dev. Neurosci.* 6:553–565.
54. Swope, S.L., and R.L. Huganir. 1993. Molecular cloning of two abundant protein tyrosine kinases in *Torpedo* electric organ that associate with the acetylcholine receptor. *J. Biol. Chem.* 268:25152–25161.
55. Swope, S.L., S.J. Moss, C.D. Blackstone, and R.L. Huganir. 1992. Phosphorylation of ligand-gated ion channels: a possible mode of synaptic plasticity. *FASEB J.* 6:2514–2523.
56. Sytkowski, A.J., Z. Vogel, and M.W. Nirenberg. 1973. Development of acetylcholine receptor clusters on cultured muscle cells. *Proc. Natl. Acad. Sci. USA*. 70:270–274.
57. Valenzuela, D.M., T.N. Stitt, P.S. DiStefano, E. Rojas, K. Mattsson, D.L. Compton, L. Nuñez, J.S. Park, J.L. Stark, D.R. Gies, et al. 1995. Receptor tyrosine kinase specific for the skeletal muscle lineage: expression in embryonic muscle, at the neuromuscular junction, and after injury. *Neuron*. 15:573–584.
58. Wallace, B.G. 1995. Regulation of the interaction of nicotinic acetylcholine receptors with the cytoskeleton by agrin-activated protein tyrosine kinase. *J. Cell Biol.* 128:1121–1130.
59. Wallace, B.G., Z. Qu, and R.L. Huganir. 1991. Agrin induces phosphorylation of the nicotinic acetylcholine receptor. *Neuron*. 6:869–878.
60. Weldon, P.R., F. Moody-Corbett, and M.W. Cohen. 1981. Ultrastructure of sites of cholinesterase activity on amphibian embryonic muscle cells cultured without nerve. *Dev. Biol.* 84:341–350.
61. Zhang, Z.Y., J.C. Clemens, H.L. Schubert, J.A. Stuckey, M.W. Fischer, D.M. Hume, M.A. Saper, and J.E. Dixon. 1992. Expression, purification, and physicochemical characterization of a recombinant Yersinia protein tyrosine phosphatase. *J. Biol. Chem.* 267:23759–23766.
62. Zhao, Z.Z., Z.J. Tan, C.D. Diltz, M. You, and E.H. Fischer. 1996. Activation of mitogen-activated protein (MAP) kinase pathway by pervanadate, a potent inhibitor of tyrosine phosphatases. *J. Biol. Chem.* 271:22251–22255.